DOI: 10.13009/EUCASS2023-901
Aerospace Europe Conference 2023 – 10TH EUCASS – 9TH CEAS

Improving cooling channel heat transfer via femtosecond laser texturing

Frederik Mertens[1†], *Balasubramanian Nagarajan*[2], *Sylvie Castagne*[2], *Maria Rosaria Vetrano*[1] *and Johan Steelant*[3]
[1] *KU Leuven, Department of Mechanical Engineering, Division of Applied Mechanics and Energy Conversion* (TME), Heat and Mass Transfer group, B-3001 Leuven.
[2] *KU Leuven, Department of Mechanical Engineering, Division of Manufacturing Processes and Systems* (MaPS) and Flanders Make@KU Leuven M&A, B-3001 Leuven.
[3] *ESA, Flight Vehicles and Aerothermodynamics Engineering Section (TEC-MPA), ESTEC, NL-2200 Noordwijk.*
frederik.mertens@kuleuven.be
[†]Corresponding author

Abstract

Efficient cooling using boiling heat transfer is crucial in space applications for thermal management systems. Further heat transfer enhancements can be achieved by functionalizing the solid surface with specific micro-/nano textures, thus increasing the amount and performance of nucleation sites. In this paper, we investigate the impact of femtosecond laser texturing on heat transfer coefficients and bubble dynamics during flow boiling in a 5x5mm channel using a thermosensitive fluid, i.e., HFE7000. We will show that the enhancement obtained (about 25%) strongly decreases with time due to fluid degradation.

1. Introduction

It is a fact that the development of efficient cooling-heating devices is a crucial requirement in many applications, among which, for example, microelectronics[1] and aerospace engineering[2] . The rapid increase in transistor packing and the continuous decrease in component size have led to a strong need for thermal packaging and management. One could point to a trend of exponential increase in heat flux at the chip level.[3] Unfortunately, today's use of strong power density is coupled with a lack of efficient heat dissipation methods leading to a truly technological bottleneck. Therefore, understanding the transport phenomena involved in micro heat transfer and their enhancement is definitely needed to allow further technological miniaturization steps. Especially in the vacuum of space, e.g., with growing satellite power densities, compact heat evacuation becomes even more challenging.

Flow boiling demonstrates significantly higher heat transfer performance than conventional single-phase cooling methods because of the latent heat of the fluid being utilized. As the coolant fluids are in direct contact with heat-producing electronics, often dielectric fluids such as fluorocarbon fluids (FC-72, FC-87, and PF-5060) and hydrofluoroethers (HFE-7000, HFE-7100, HFE-7300) are the fluids of choice due to their electrical insulation, chemical compatibility, high dielectric strength, inertness, stability, non-flammability, and non-reactivity. Furthermore, these fluids commonly have a low boiling point, making extracting heat at lower temperatures easier and preserving temperatures within a recommended range for the specific application or device. However, naturally having a low surface tension and a high degree of wettability enables the fluid to penetrate deep into boiling cavity sites, often resulting in higher needed incipient superheats than a conventional fluid such as water. As shown in Table 1, their thermophysical properties, such as the latent heat of vaporization and the liquid's specific heat, are also poorer than those of water. They also possess a high air solubility (for example, 31% by volume at 1 atm and $25°C$ for 3 M's HFE-7000[4]). This high solubility can result in artificial boiling incipience even well below the saturation temperature of the pure fluid because dissolved gas is released. Therefore, thorough degassing of these fluids before final use in the system is essential. Lastly, because of their high wettability, they are prone to leaks more easily.

Despite these fluids' poor thermophysical properties, surface functionalization can be employed to enhance the boiling heat transfer with dielectric fluids at the fundamental scale, directly impacting nucleation. Many surface modification techniques have already been developed and investigated. Direct coating methods such as electrochemical deposition[5] , chemical vapor deposition[6] , and direct powder sintering[7] have been studied, and remarkable enhancements in boiling heat transfer coefficients and critical heat fluxes were reported. On the other hand, intrinsic surface features developed

DOI: 10.13009/EUCASS2023-901

Table 1: Thermophysical properties of selected dielectric fluids (from 3M datasheets) and water at 1 atm and 25 $°C$

	FC-72	FC-87	HFE-7000	HFE-7100	HFE-7300	Water
Boiling point ($°C$)	56	30	34	61	98	100
Liquid density (kg/m^3)	1680	1650	1400	1510	1660	997
Liquid dynamic viscosity (kg/ms)	6.4×10^{-4}	4.5×10^{-4}	4.5×10^{-4}	5.8×10^{-4}	11.8×10^{-4}	8.9×10^{-4}
Liquid specific heat (J/kgK)	1100	1100	1300	1183	1140	4182
Liquid thermal conductivity (W/mK)	0.057	0.056	0.075	0.069	0.063	0.61
Latent heat of vaporization (kJ/kg)	88	103	142	112	102	2257
Liquid surface tension (mN/m)	10.0	9.0	12.4	13.6	15.0	72.0

using MEMS/NEMS technologies[8] , additive manufacturing (AM)[9] , and other advanced manufacturing techniques have also achieved significant boiling heat transfer augmentation. However, despite the degrees of boiling enhancement, a common factor here is the scalability of these techniques to produce enhanced surfaces on a larger scale and economically. More recently, femtosecond laser processing has provided the possibility of finally achieving this goal as well[10] .

The use of micro/nano-structured surfaces associated with the local characterization of the wall surface temperature and the visualization of the two-phase flow behavior is necessary to improve our knowledge of the basic mechanisms and their modeling. This will fill the current knowledge gap, which is related, on the one hand, to the absence of reliable boiling models that account for micro-scale phenomena and, on the other hand, to the lack of predictive tools for the flow boiling enhancement obtained using these surfaces.

2. Boiling terminology

Some fundamental boiling terminology and physical quantities are briefly summarised below.

2.1 Heat transfer coefficient

A quantitative measure of the heat transfer between a surface at temperature T_s and a fluid at T_f in the bulk is defined as a heat transfer coefficient (HTC) h:

$$h = \frac{q}{T_s - T_f} \tag{1}$$

where q corresponds to the imposed heat flux through the surface. The local HTC will differ from point to point in the flow as boundary conditions change. An overall averaged HTC can also be defined.

2.2 Bubble nucleation

As the temperature of a heating surface is increased, there will be a moment where vapor bubbles start to form and escape from certain preferred spots on the surface (*Onset of nucleate boiling*). The spots where these bubbles grow are called *nucleation sites*. These inclusions are too small to allow liquid to enter because of the liquid surface tension and are filled with gas (vapor or non-condensable gas). These residual vapor pockets act as sites for bubble inception. Some further terms used to describe nucleation performance include the *nucleation site density* (n) on a given surface area, the *bubble departure diameter* (D), and the *bubble departure frequency* (f). The Heat Transfer Coefficient (HTC) scales with these parameters, e.g. Mikic and Rohsenow[11] described the relation HTC = $CnD^2 f^{(1/2)}$ for pool boiling where C also includes fluid density, thermal conductivity and specific heat.

2.3 Boiling curves

Boiling performance is often characterized in the form of boiling curves. These curves show the relation between the heat flux and surface temperature. Usually, the temperature is given as an excess over the fluid saturation temperature. An example can be seen in Figure 1. It is apparent that there are multiple regions within this curve. For most practical engineering applications, only the nucleate boiling region is of interest since it corresponds to a high heat removal rate at low surface temperatures. This regime goes from the onset of nucleate boiling to the critical heat flux (CHF), point

DOI: 10.13009/EUCASS2023-901

A to point C in Figure 1. Boiling enhancement is associated with shifting the boiling curve to the left (enhanced HTC and earlier onset of nucleate boiling) and upwards (enhanced CHF).

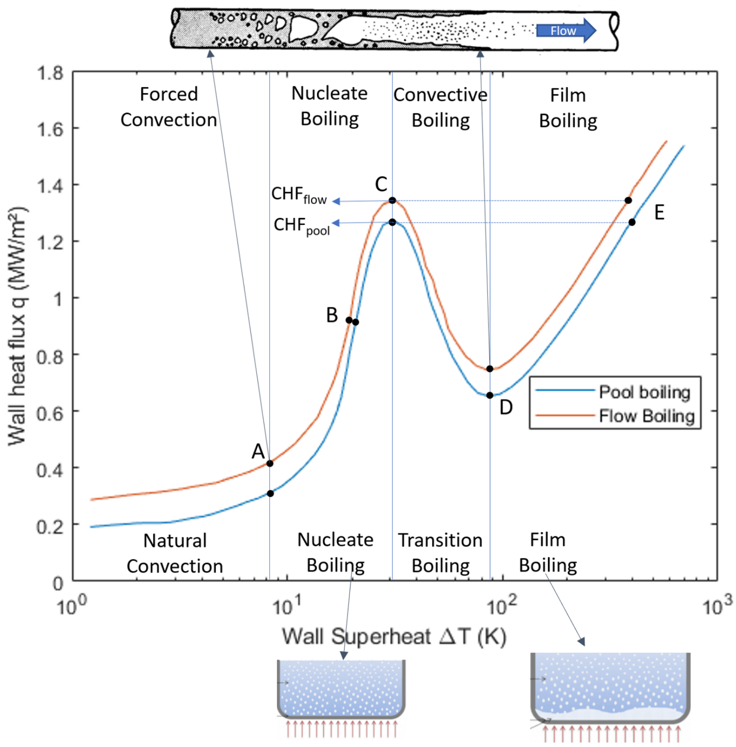

Figure 1: Flow vs Pool boiling curve for saturated water at 1atm[12]

2.4 Critical heat flux (CHF)

The critical heat flux is defined as the heat flux where there are so many bubbles on the wall simultaneously that they merge into a continuous but unstable vapor film that covers parts of the surface as a blanket of gas. This point is also called burnout or boiling crisis. So, the CHF represents the maximum heat flux that can be attained in most applications since, after this point, a slight increase in heat flux corresponds to a very high rise in surface temperature, which could lead to severe damage in most cases. This is also illustrated in the boiling curves in Figure 1, where there is a jump from point C to point E after reaching the CHF.

2.5 Flow Boiling

Expanding on conventional forced convective heat transfer, *Flow boiling* refers to a case where a liquid is pumped through a system and boiled. Due to additional convection, nucleate flow boiling heat transfer can exceed that of pool boiling. An example of a comparison between the pool and flow boiling curves is given in Figure 1 for saturated water. However, compared to pool boiling, flow boiling is affected by additional factors such as mass flux and vapor quality. Furthermore, including a pump also creates additional system complexity, and pressure drop becomes an important factor. Two heat transfer modes are commonly observed in flow boiling processes, nucleate boiling-dominated and convection-dominated. In the nucleate boiling-dominated mode, the heat transfer coefficient changes significantly based on the heat flux. In contrast, in the convection-dominated mode, the mass flux and vapor quality act as the main effects on the heat transfer coefficient. Flow boiling can also be divided into different flow pattern regimes, for example, bubbly flow, plug/slug flow, and annular flow, as shown in Figure 2. Many researchers have presented correlations to predict flow boiling heat transfer performance and pressure drop. For example, Kandlikar[13] developed a general correlation for saturated two-phase flow boiling heat transfer inside horizontal and vertical tubes using a wide range of experimental data and ten different fluids and Thome et al.[14] presented two-phase pressure drops and flow patterns of ammonia and hydrocarbons applied in air-conditioning, refrigeration, and heat pump systems.

DOI: 10.13009/EUCASS2023-901

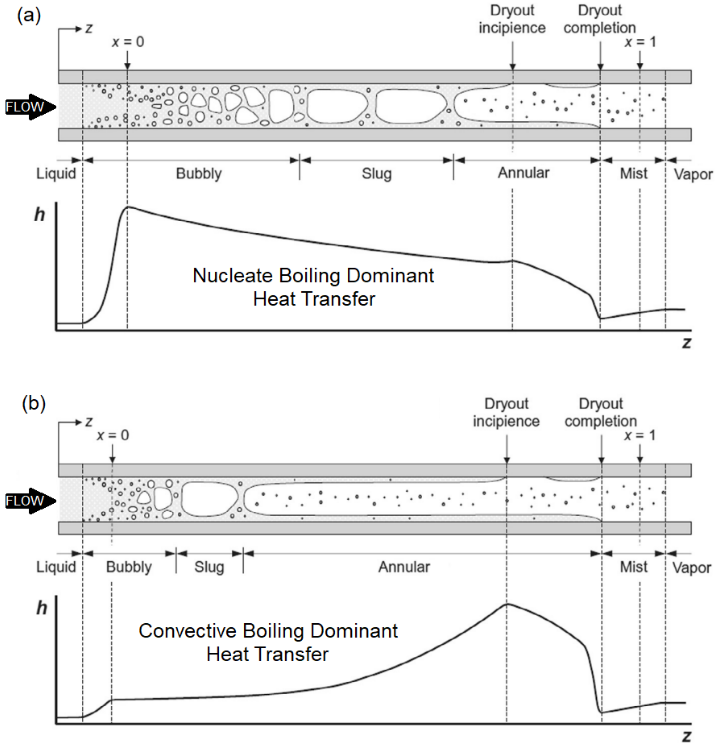

Figure 2: Schematics of flow regimes, wall dryout and variation of heat transfer coefficient along an uniformly heated channel for **(a)** nucleate boiling dominant heat transfer and **(b)** convective boiling dominant heat transfer[15]

An overview of the parameters that have a direct influence on the flow boiling process in a given physical channel consists of:

- **Heat flux:** Since most applications are heat-flux controlled, this directly influences the boiling regime observed.
- **Subcooling:** The degree of subcooling is defined as the temperature difference between the actual fluid temperature and the fluid's saturation temperature at the same pressure, where the actual temperature is lower than the saturation temperature.
- **Mass flow rate:** In flow boiling, fluid is being pumped through the system. The mass flow rate thus has a significant impact on the heat transfer as well as a direct impact on the bubble dynamics.
- **Fluid choice:** When it is required to increase the heat transfer in a given system, a good choice of working fluid is the first step to take. Over the years, many fluids have been engineered to be employed in a multitude of applications.
- **Surface functionalization:** The area of surface modification for boiling heat transfer enhancement has become more and more investigated in the last years. By modifying the heated surface with micro- and nanostructures, cavities are created that make it easier for the bubbles to grow and detach, thus improving the heat transfer at the core mechanisms. Textured surfaces include, e.g., porous foams,[16] wettability modifying coatings,[17] micro pin fins,[18] artificial cavities,[19] and much more.

3. Femtosecond laser texturing

3.1 Background

Laser Beam Machining (LBM) is a mature technology by now, widely used in manufacturing.[20] In general, a high power density of the laser beam makes it able to remove material by melting and vaporization from a workpiece that absorbs the thermal energy deposited. As LBM is a non-contact machining method, there are no cutting forces or tool wear, and the workpiece is protected from mechanically induced damage, contamination, and machine vibration. This

DOI: 10.13009/EUCASS2023-901

makes LBM a flexible process that depends on the thermal and optical properties rather than the mechanical properties of the material being machined.[21]

The development of ultrashort pulse lasers (typically less than 10 picoseconds) demonstrates great potential to fabricate fine micro/nanoscale features on a wide variety of materials due to high peak power, low ablation thresholds, minimized heat-affected zone and minimized thermal stress. This is due to the "cold" ablation as the pulse duration is shorter than the electron-phonon relaxation time. Effectively, femto-second laser texturing can be considered as an athermal process, as the material is instantly vaporized before heat has the chance to be transferred into the material. This is contrary to the more conventional (thermal) laser processing techniques where a longer pulse also generates effects to the surrounding area, even damaging it.

Process control parameters include scanning speed (mm/s), pulse energy (μJ), spot size (μm), pulse pitch distance (μm), pulse duration (fs), pulse repetition rate (kHz), inclination angle (°) and the number of passes (#). With proper control, desired features are achieved with varying diameter/width, depth, inclination, and spacing.

3.2 Fabrication and characterization of textures

Femtosecond laser texturing experiments on the flow boiling test sections were performed using a facility available at KU Leuven (FemtoFac). It consists of a multi-axes micromachining platform equipped with a 5-axes mechanical air bearing stage, a 2-axes optical galvo-scanner and a femtosecond laser source (CARBIDE, Light conversion) with the following specifications: pulse duration - 250 fs to 10 ps, wavelength - 1030 nm, 515 nm, 355 nm; maximum average power - 20 W, frequency - 1 MHz, maximum pulse energy - 400 μJ. Figure 3 shows a boiling test section mounted on the motion stages of the femtosecond laser machine.

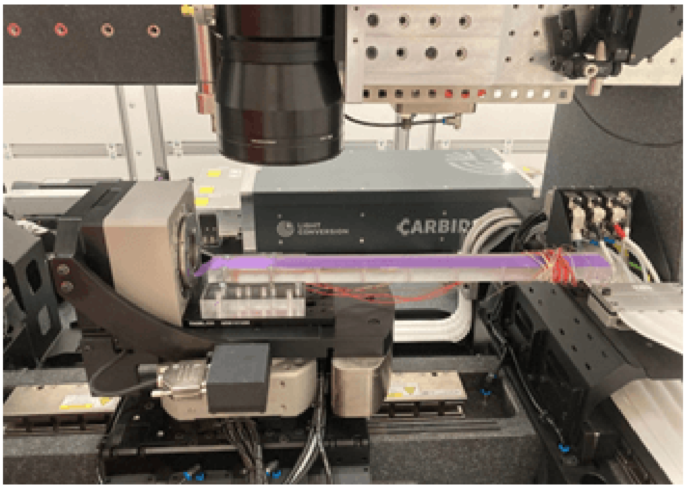

Figure 3: Experimental setup for femtosecond laser texturing of flow boiling test sections

The textures were fabricated on the flow boiling test section over an area of 82 mm x 7 mm using the following laser parameters: pulse duration = 250 fs, spot size ~ 20 μm, pulse energy = 15 μJ, scanning speed = 300 mm/s, number of scanning passes = 3, cross-hatching scanning strategy with a hatch spacing of 50 μm. The topography of the fabricated textures is characterized using a Sensofar optical profiler and scanning electron microscopy whereas EDX analysis performed to analyze the chemical composition.

4. Experimental Flow Boiling Setup

In order to assess the flow boiling performance in earth gravity, a fluidic loop was constructed as shown in Figure 4. The loop consists of a magnetically driven gear pump that is linked via PID to a Coriolis mass flow meter, a filter circuit to remove any entrained dust or particles, a tube & shell heat exchanger connected to a thermal bath acting as preheater to set the test section inlet temperature, a boiling test section, a radiator fan assembly to remove heat, a membrane accumulator to stabilize the system pressure, a programmable power supply to provide the boiling heater power, a high speed camera for bubble visualization and a data acquisition system. The test section consists of a plexiglass outer shell forming a 5x5mm channel with an embedded film heater, distributed thermocouples, and pressure transducers.

DOI: 10.13009/EUCASS2023-901

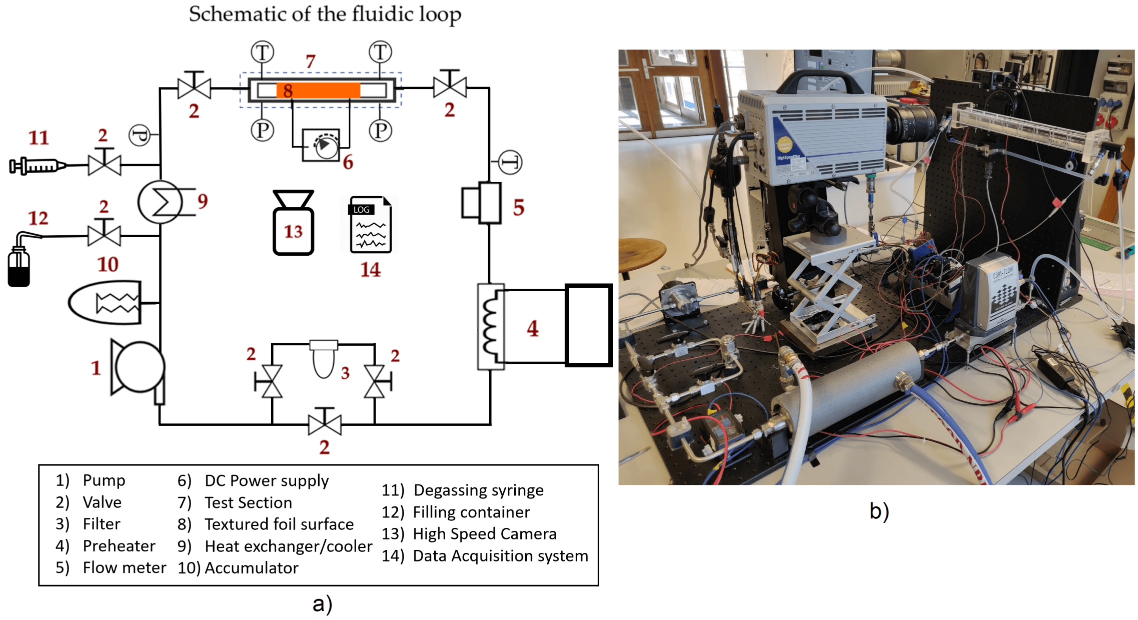

Figure 4: a) Schematic b) test setup for flow boiling experiments

The surfaces include 200 μm thick copper and stainless steel foils. The test section is mounted on a 360° rotatable platform allowing to be able to investigate the effect of the gravity vector. LED backlighting provides illumination for the high speed camera visualizations. Another small camera monitors the boiling process from above. The available development length is approximately 300mm, meaning that up to $Re = 1200$, the flow can be considered developed in the laminar regime. The heated length is approximately 100mm. A closer view of the test section is shown in Figure 5.

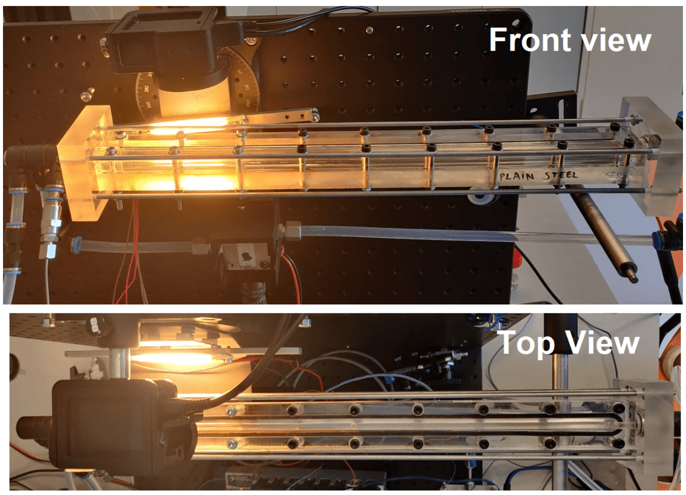

Figure 5: Test section front and top close-up

The working fluid for this study initially was HFE7000. It is a dielectric liquid with a saturation temperature of 34°C at 1 bar, making it easier to observe boiling phenomena, as not much additional power is required. Because of reasons that will be discussed in the next section, a change in working fluid had to be made. After careful consideration and testing, FC-72 (Perfluoro-hexane, C6F14) was chosen as the replacement. C6F14 has a saturation temperature of 57°C at 1 bar, so more power is needed for heating compared to HFE7000.

More regarding space applications, another setup is in the process of construction that will be used for microgravity tests onboard parabolic flights. The main difference here is that there will be two test sections in series, in order to compare textured to plain surfaces simultaneously at the exact same gravity level. These flights are planned for November 2023 and will use a selection of promising textures from further on-ground testing.

DOI: 10.13009/EUCASS2023-901

5. Preliminary results

5.1 Methodology

A consequence of the laser-matter interaction in femtosecond laser texturing is the creation of a submicron periodic structure called Laser Induced Periodic Surface Structures (LIPSS) in addition to any larger microstructures created. LIPSS are expected to have a large impact on the heat transfer enhancement because of the increased wetting and capillary wicking capabilities and increased active nucleation sites with the used highly wetting dielectric fluids. Since LIPSS will always be present, it is needed to thoroughly characterize their influence first, before investigating the larger scale textures (grooves, pillars, holes...). Of course, texture performance is also related to system operating conditions, so the effects of inlet subcooling, flow rate/Reynolds number, and channel inclination are observed. The channel inclination is observed to capture the influence of the gravity component perpendicular to the surface in order to get an idea of the surface performance in microgravity. In principle, a produced texture would only show best performance for those specific operating conditions it would be designed for. For this reason, the relation between texture geometry and heat transfer is investigated with the prospect of creating a data-driven modeling database in the future.

For reference in the presented curves in this section, the letter-number combinations refer to the selected operating conditions, with the letter representing the channel inclination and the number representing the combination of Reynolds number and inlet subcooling for the given experiment. For example, a horizontal upwards facing heater (A) test matrix would be as presented in Table 2 below.

Table 2: Example test matrix for horizontal upwards heater as clarification for presented curves

Re \ ΔT_{sub}	$5°C$	$10°C$	$20°C$
1200	A1	A2	A3
3600	A4	A5	A6

5.2 Flow boiling on plain surface

As a baseline, flow boiling of HFE7000 was performed on manufacturer-provided plain copper for two Reynolds numbers (1200 and 3600) and three approximate inlet subcooling values ($5°C$, $10°C$ and $20°C$) for each of the investigated channel inclinations (Horizontal, ±45° with upwards facing heater, vertical up- and downflow, and horizontal downwards facing heater). Some HTC curves for a specific point on the surface are given in Figure 6 and show that HTC increases with increasing Re and decreasing inlet subcooling and show that vertical upflow is most efficient at bubble evacuation, which is in line with expectation.

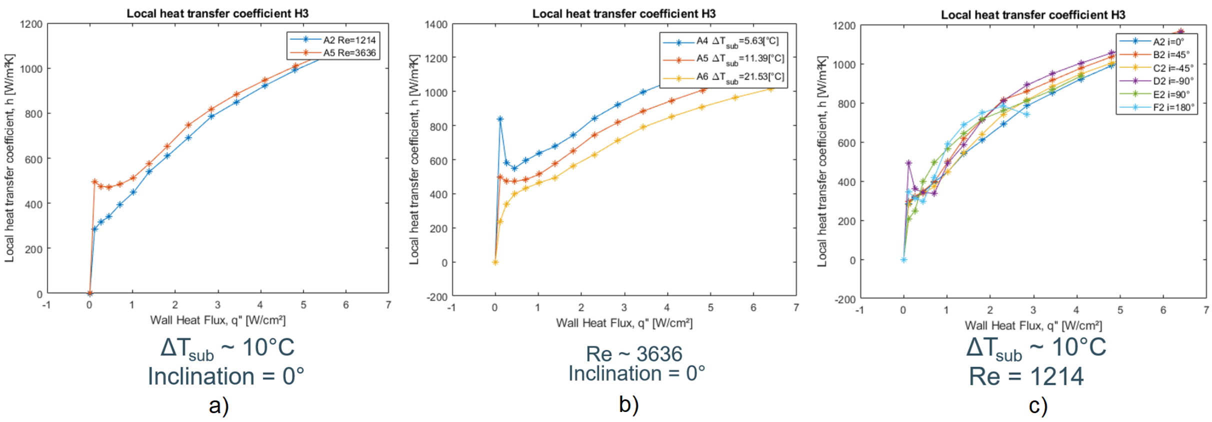

Figure 6: Effect of a) Re, b) Inlet subcooling and c) channel inclination on HTC curves on plain copper

DOI: 10.13009/EUCASS2023-901

5.3 Flow boiling on textured surface

The HTC curve obtained using a plain copper surface was compared to what was measured with a copper textured sample having mostly LIPSS on the surface as a by-product of creating a shallow grooved pattern. The test surface can be seen in Figure 7 as measured by an optical profilometer and a scanning electron microscope (SEM).

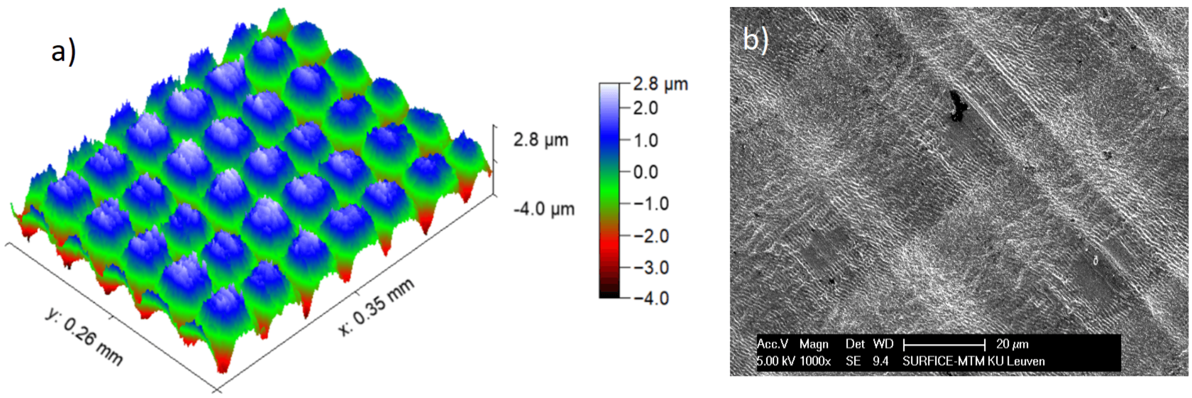

Figure 7: a) Optical profilometer surface morphology of grooved textured surface b) LIPSS SEM image

Perpendicular grooves with an average depth of $3.63 \pm 0.47\ \mu m$ were fabricated on the copper foils following a $50\ \mu m$ spacing. As the SEM image shows, laser-induced periodic surface textures (LIPSS) with a submicron scale periodicity were formed superposed on the created grooves, creating hierarchical multiscale surface textures.

First experiments with this LIPSS-dominated structure showed HTC enhancement of 25% over the smooth sample at Re=3600 and inlet subcooling of $10°C$, as is also shown in Figure 8 a). However, due to fluid degradation, the enhancement was short-lived and was gradually completely nullified after three 1.5h experimental runs, as shown in Figure 8 b) and c). After some more runs, the performance stabilized, showing no more changes over time.

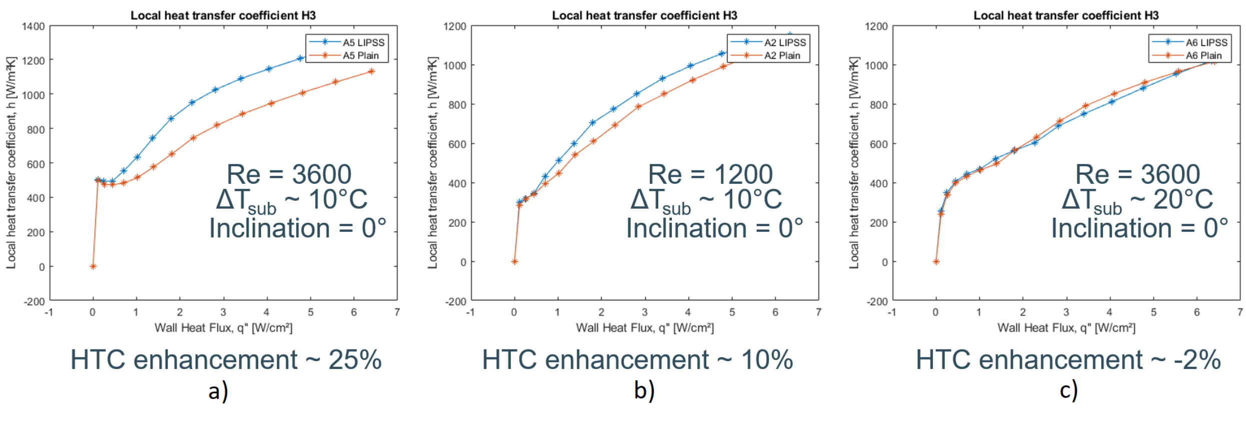

Figure 8: HTC enhancement of textured surface wrpt plain copper surface in three consecutive experimental runs a, b) and c)

The enhancement observed in the initial experimental run shows the potential of LIPSS textures to enhance the HTC. The reason for the performance degradation is entirely related to the fluid, HFE7000, and will be discussed in the following section. The initial enhancement due to the textures can also be observed from bubble visualization, as shown in Figure 9 for the given operating conditions. As an overall observed trend, (fresh) textures/LIPSS produce more bubbles and generally smaller bubbles with a higher departure frequency and lead to an onset of nucleate boiling at a lower surface temperature. The enhancement in HTC is thus clearly motivated.

DOI: 10.13009/EUCASS2023-901

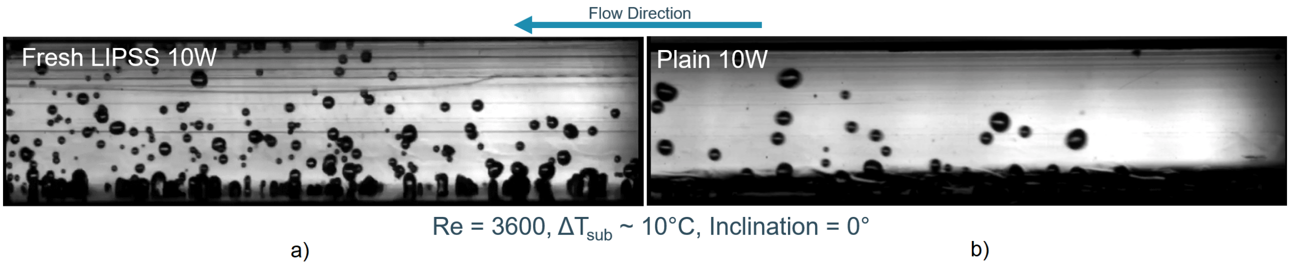

Figure 9: Bubble visualization at similar conditions for fresh a) textured and b) plain surface

5.4 HFE7000 - Degradation

As mentioned in the section addressing textured boiling, the enhanced HTC was quickly declining over some experimental runs, getting completely nullified to even worsened. Also, using the plain sample, something similar was observed, but this time slightly enhancing the performance over a much longer period of experimental run time. The over time quasi-stabilized HTC curves for both surfaces are compared to their fresh values in Figure 10 where "N" stands for the new stabilized curve. It can be seen that the performance of the plain surface increases while the textured performance decreases even slightly below the stabilized plain surface curve.

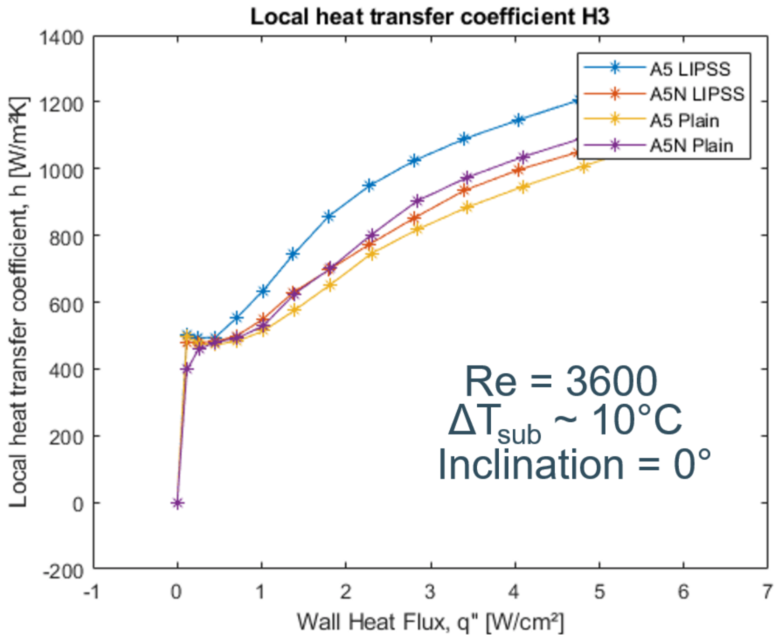

Figure 10: Comparison of boiling curves for fresh and stabilized (N) plain and textured surfaces.

The effect on the bubble dynamics of LIPSS degradation can also be seen in Figure 11. In general, the degradation results in fewer bubbles, bigger bubbles, and a later onset of nucleate boiling.

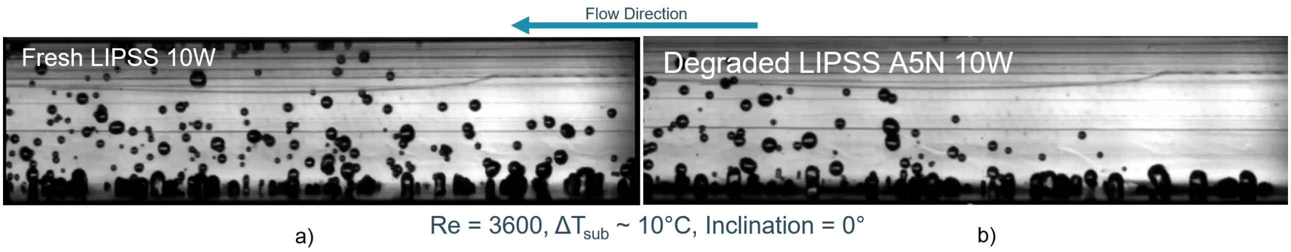

Figure 11: Bubble visualisation at same conditions for a) fresh textures and b) degraded textures

DOI: 10.13009/EUCASS2023-901

The reason for this degradation (or enhancement in the plain case) becomes clear when observing the surface over time from above. Figure 12 shows some pictures of the textured surface over operating time.

Figure 12: LIPSS surface degradation over time

Black spots and streaks are observed to appear, affecting the nucleation process by deactivating and degrading the cavities created by the femtosecond laser. These streaks are seen to appear and grow/thicken more and more over time. The same happens for the plain surface, but here, due to a lack of predetermined nucleation sites, the streaks take quite a bit longer to appear and grow compared to the LIPSS case. A degraded plain surface can be seen in Figure 13.

Figure 13: Plain copper surface degraded over time

These spots could be mostly cleaned (using isopropanol or HFE7000) from the surface, but with copper, there was some residual damage left on the surface which could not be cleaned, showing permanent damage to the boiling surface, possibly due to oxidation at the black spot sites.

Several possible reasons for the appearance of these black spots were investigated. It was found that they were not due to the components/materials used in the setup and not related to the boiling surface material. The same degradation was also observed on plain stainless steel, as shown in Figure 14. The only difference between copper and steel was that, with steel, the spots could be cleaned off without detecting underlying damage to the surface (no oxidation effects).

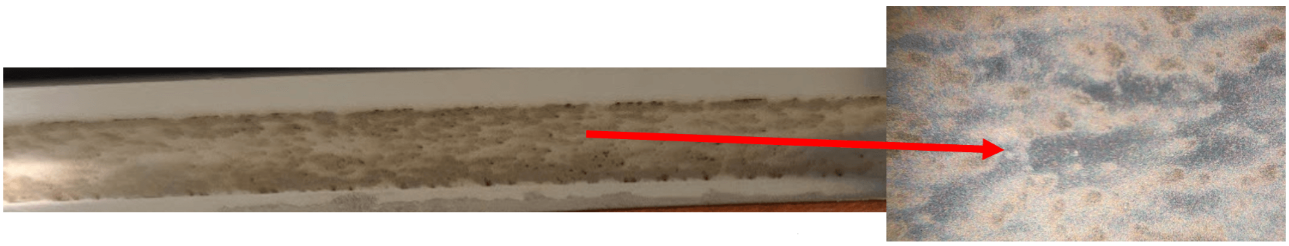

Figure 14: Plain stainless steel surface degraded over time

Further investigation was done into the chemical composition of the spots using energy-dispersive X-ray spectroscopy, from which some results are shown in Figure 15. The spots were found to consist mostly of carbon, oxygen, and fluor, which are all components of HFE7000 ($C_3F_7OCH_3$), the used working fluid.

DOI: 10.13009/EUCASS2023-901

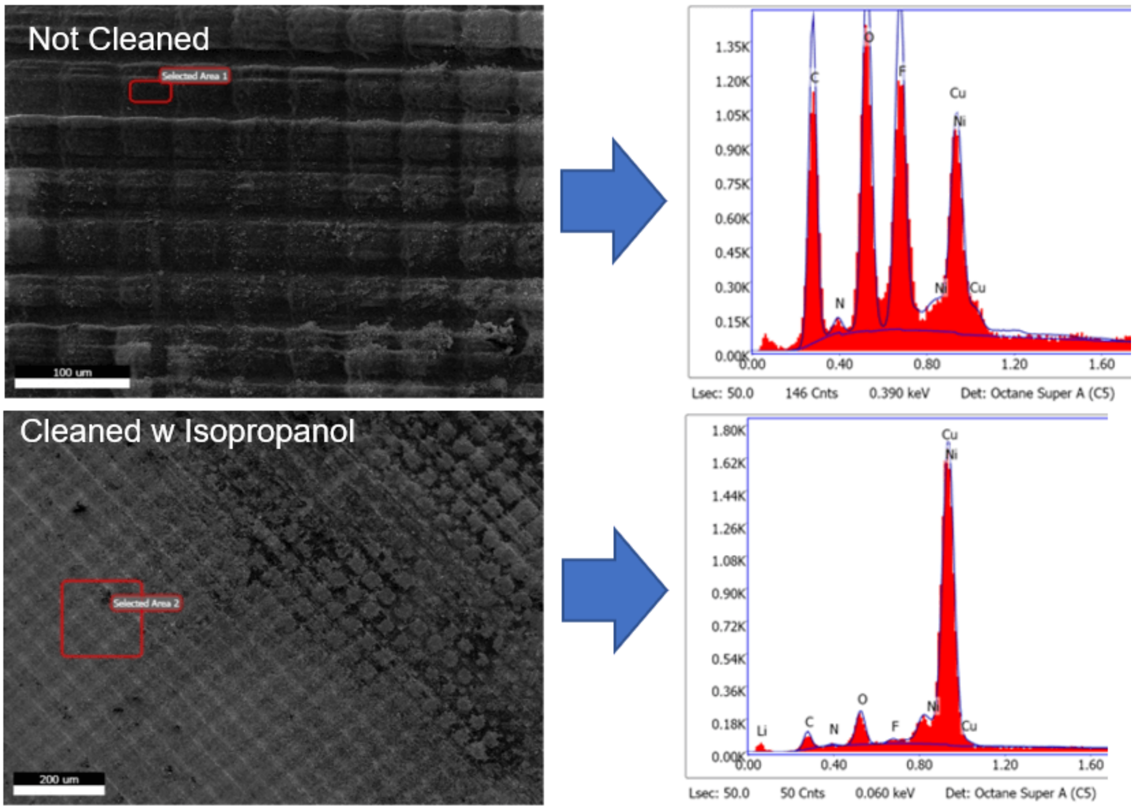

Figure 15: Black spot spectroscopy data for non-cleaned and cleaned sample

For this reason, HFE7000 was abandoned as working fluid as nothing truly useable can ever be said about the texture performance when using it. Similar spots were found using HFE-7200 and Novec-649 in pool boiling. FC-72 was the only fluid that did not show any degradation during both pool and flow boiling campaigns and has been chosen as the best working fluid alternative. However, it is currently difficult to find more FC-72 since production of the 3M fluor line (Novec, HFE, FC,...) is permanently halted due to the "PFAS" stop. Another still easily available FC-72 alternative is Flutec PP1, which has approximately identical properties. Both fluids are perfluoro-hexane (C_6F_{14}), in a different isomer, as shown in Figure 16. While isomers can usually exhibit great differences in thermophysical and chemical properties, these two are one of the few that actually don't differ much at all. The main reason is thought to be because both molecules are filled with Fluorine everywhere. Fluorine has the highest electronegativity of all elements, thus creating very steady electron clouds around it. This suggests that the interactions between Fluorine atoms from different molecules will dominate the intermolecular weak forces instead of the extra branch of the carbon chain or the steric hindrance resulting from the overall molecule shape change. New tests are currently being performed using FC-72 and PP1.

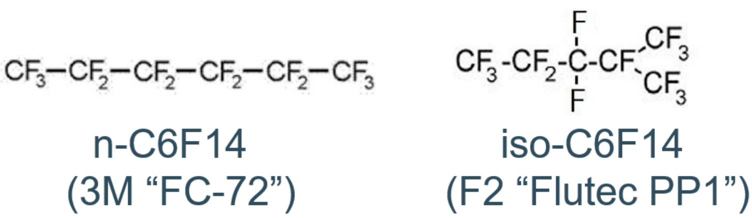

Figure 16: FC-72 (n-PFH) and PP1 (iso-PFH) isomers of C_6F_{14}

DOI: 10.13009/EUCASS2023-901

6. Conclusion

In this paper, ongoing works were presented with the goal of obtaining data concerning the relation between Laser Induced Periodic Surface Structures (LIPPS), obtained by texturing shallow grooves, and the resulting boiling heat transfer performance of dielectric fluids, with an aim of creating and understanding more specialized hierarchical surface structures in the future. The capabilities of the femtosecond laser are very promising, allowing much freedom in the cavity design. An earth gravity flow boiling setup is operational, allowing also investigation of the gravity direction influence. A parabolic flight experiment is currently being designed to assess the performance in microgravity environment of selected produced textures. LIPSS-dominant copper textures were tested with HFE7000. An initial 25% improvement in HTC was observed, but soon declined and worsened over time. This degradation was found to be caused by deposition products from HFE-7000, rendering any surface texturing useless in due time. A change in the operating fluid was made from the more green (ultra-low global warming potential, GWP=1) and easier to boil (saturation temperature of 34°C) HFE-7000 to the less green (GWP=7400) and somewhat more difficult to boil (saturation temperature of 57°C) perfluoro-hexane (C_6F_{14}) for future boiling experiments.

7. Acknowledgments

The authors gratefully acknowledge the Fonds Wetenschappelijk Onderzoek - Vlaanderen (FWO) (Mandaat Aspirant (1S62222N) and Medium-Scale Research Infrastructure FemtoFac (I001120N)) and the European Space Agency (OSIP 4000135205/21/NL/GLC/my) for having funded the research activity. ESA's Open Space Innovation Platform (OSIP) allows discovery of novel ideas and investment in new unconventional activities to foster advancement in the space industry.

References

[1] S M Sohel Murshed. Electronics cooling - an overview. *IntechOpen, Rijeka*, Chapter 1:1–2, 2016.

[2] M. Williams et al. Advanced heat exchanger technology for aerospace applications. *SAE Technical Paper 2008-01-2903*, 2008.

[3] Liming Xiu. *The Turn of Moore's Law from Space to Time*. Springer, Singapore, 2022.

[4] 3M. 3m novec-7000 engineered fluid product description.

[5] Mohamed S. El-Genk and Amir F. Ali. Enhancement of saturation boiling of pf-5060 on microporous copper dendrite surfaces. *Journal of Heat Transfer*, 132:1–9, 7 2010.

[6] Sebastine Ujereh, Timothy Fisher, and Issam Mudawar. Effects of carbon nanotube arrays on nucleate pool boiling. *International Journal of Heat and Mass Transfer*, 50:4023–4038, 9 2007.

[7] Tae Young Kim, Justin A. Weibel, and Suresh V. Garimella. A free-particles-based technique for boiling heat transfer enhancement in a wetting liquid. *International Journal of Heat and Mass Transfer*, 71:808–817, 4 2014.

[8] J. J. Wei, L. J. Guo, and H. Honda. Experimental study of boiling phenomena and heat transfer performances of fc-72 over micro-pin-finned silicon chips. *Heat and Mass Transfer/Waerme- und Stoffuebertragung*, 41:744–755, 6 2005.

[9] M. Wong, I. Owen, C. J. Sutcliffe, and A. Puri. Convective heat transfer and pressure losses across novel heat sinks fabricated by selective laser melting. *International Journal of Heat and Mass Transfer*, 52:281–288, 1 2009.

[10] Rebeca Martinez Vazquez, Francesca Bragheri, and Petra Paie. *New Trends and Applications in Femtosecond Laser Micromachining*. MDPI, Basel, 2022.

[11] B.B. Mikic and W.M. Rohsenow. A new correlation of pool-boiling data including the effect of heating surface characteristics. *Journal of Heat Transfer*, 91(2):245–250, 1969.

[12] Nukiyama Shiro. The maximum and minimum values of the heat q transmitted from metal to boiling water under atmospheric pressure. *International Journal of Heat and Mass Transfer*, 27:959–970, 1984.

[13] S G Kandlikar. A general correlation for saturated two-phase flow boiling heat transfer inside horizontal and vertical tubes. *Journal of Heat Transfer*, 112:219–228, 2 1990.

DOI: 10.13009/EUCASS2023-901

[14] John R. Thome, Lixin Cheng, Gherhardt Ribatski, and Luiz F. Vales. Flow boiling of ammonia and hydrocarbons: A state-of-the-art review. *International Journal of Refrigeration*, 31:603–620, 6 2008.

[15] Sung Min Kim and Issam Mudawar. Review of databases and predictive methods for heat transfer in condensing and boiling mini/micro-channel flows. *International Journal of Heat and Mass Transfer*, 77:627–652, 2014.

[16] I. Pranoto and K. C. Leong. An experimental study of flow boiling heat transfer from porous foam structures in a channel. *Applied Thermal Engineering*, 70:100–114, 9 2014.

[17] Jee Hyun Seong, Chi Wang, Bren Phillips, and Matteo Bucci. Effect of pvd-coated chromium on the subcooled flow boiling performance of nuclear reactor cladding materials. *Applied Thermal Engineering*, 213, 8 2022.

[18] Aixiang Ma, Jinjia Wei, Minzhe Yuan, and Jiabin Fang. Enhanced flow boiling heat transfer of fc-72 on micro-pin-finned surfaces. *International Journal of Heat and Mass Transfer*, 52:2925–2931, 6 2009.

[19] Jure Voglar, Peter Gregorcic, Matevz Zupancic, and Iztok Golobic. Boiling performance on surfaces with capillary-length-spaced one- and two-dimensional laser-textured patterns. *International Journal of Heat and Mass Transfer*, 127:1188–1196, 12 2018.

[20] Avanish Kumar Dubey and Vinod Yadava. Laser beam machining-a review. *International Journal of Machine Tools and Manufacture*, 48:609–628, 5 2008.

[21] J. C. Ion. *Laser Processing of Engineering Materials*. Elsevier Butterworth-Heinemann, 139-178, 2005.